

# An Experimental Investigation on the Performance and the Wake Characteristics of a Wind Turbine Subjected to Surge Motion

Morteza Khosravi<sup>1</sup>, Partha Sarkar<sup>2</sup> and Hui Hu<sup>3</sup>(✉)

*Iowa State University, Ames, Iowa, 50010, USA.*

There are many advantages of floating wind turbines in deep waters, however, there are also significant technological challenges associated with it too. The dynamic excitation of wind and waves will induce excessive motions along each of the 6 degrees of freedom (6-DOF) of the floating platforms. These motions will then be transferred to the turbine, and directly impact the turbines' performance and loadings. Advanced diagnostic technique methods were employed in order to elucidate the underlying physics of a wind turbine subjected to surge motion. In the absence of a combined wind-wave basin, and in order to replicate the dynamics of the surge motion of a floating offshore wind turbine (FOWT), a 1:300 scaled model wind turbine was installed on a high precision 3-DOF motion simulator device in a well-controlled, closed loop, dry-boundary layer wind tunnel. The inflow conditions of the wind tunnel were matched to that corresponding to the deep-water offshore environment. A Froude scaling method was employed in order to obtain the correct forces and responses on the floating turbine. In the case of the surge motion and in comparison with a traditional bottom-fixed turbine, the results of the wake study does show slight decrease in the entrainment of the turbulent kinetic energy from the high energy flow above the turbine. A slight increase in power output was also noted.

## I. Introduction

Offshore wind energy is one of the most abundant and promising sources of energy that can provide substantial amount of clean, domestic, and renewable energy. The United States is especially fortunate to be surrounded by vast waters on both sides of the nation. This provides a unique opportunity for offshore wind farm developments in this country. There is over 4000 GW of wind potential within 50 nautical miles of the U.S. coastlines (Musial et al, 2010), which is approximately four times the current U.S. power generation capacity. Offshore wind energy is divided into three categories, depending on the depth of water where the turbines are being installed. The depth of the water dictates the type of substructure technology needed to install offshore wind turbines. In shallow waters (0 m to 30 m), the turbines are being fixed to the sea floor by means of a monopile or gravity based foundations. In intermediate waters (30m to 60 m), the wind turbines are also being fixed to the sea floor but by different kind of substructures such as jacket or tripods. As the water depth increases beyond 60m, the cost of substructure increases substantially, making it almost economically infeasible to fix the turbines to the sea floor. Therefore, the turbines will need to be floated in deep waters.

By the end of 2013, there were 69 offshore wind farms operating in 11 European countries, yielding over 6.5 GW of electricity. All of these wind farms are located in shallow waters with depths less than 20 meters where the turbines are fixed to the sea floor (Corbetta G., 2014). Unlike the shallow European waters, the U.S. waters are, on the other hand, mostly deep (with the exception of a few regions in the East Coast and the Gulf of Mexico). Therefore, offshore wind farm development in the U.S. will most likely be based on the floating concept. The

---

<sup>1</sup> Graduate Student, Department of Aerospace Engineering.

<sup>2</sup> Professor, Department of Aerospace Engineering

<sup>3</sup> Professor, Department of Aerospace Engineering, AIAA Associate Fellow, Email: [huhui@iastate.edu](mailto:huhui@iastate.edu)

floating platforms that have been proposed for wind turbine applications include; semi-submersible, tension leg platform, and spar buoy.

There are many advantages of floating wind turbines in deep waters. However, there are also significant technological challenges associated with it too. Regardless of the type, floating platforms cannot easily provide high degrees of stability for mounting wind turbines. This is especially true for the Horizontal Axis Wind Turbines (HAWT) since their center of gravity (C.G.) is located at a much higher location in relation to their Center of Buoyancy (C.B.), hence, creating an unstable floating structure. There are six degrees of freedom (6-DOF) associated with any floating structures, three displacements (surge, sway, and heave) and three rotations (roll, pitch, and yaw). The dynamic excitation of wind and waves, will induce excessive motions along each of the 6-DOF's of the floating platform. These motions will then be transferred to the turbine itself, and directly impact the turbines' performance and loadings.

The study of both coupled and uncoupled motions of the floating turbines are important and necessary to determine the contributions of each motions along each of the DOFs to the overall performance, and the wake characteristics of floating wind turbines. In the current experimental study, advanced diagnostic technique methods were employed in order to elucidate the underlying physics of a wind turbine subjected to surge motion. In the absence of a combined wind-wave basin, and in order to replicate the dynamics of floating offshore wind turbines (FOWT), a 1:300 scaled model wind turbine was installed on a high precision 3-DOF motion simulator device in a well-controlled, closed loop, dry-boundary layer wind tunnel. The inflow conditions of the wind tunnel were matched to that corresponding to the deep-water offshore environment. To better understand the effects of surge motion to the overall performance and the wake characteristics of a wind turbine, the results were then compared to those of a conventional bottom fixed wind turbine.

The wake of wind turbines contains many information relevant to design and optimization of wind turbines, and hence important to study. The wake of a wind turbine is divided into near and far wake. The near wake refers to the region approximately one rotor diameter downstream of the turbine. In the near wake, the presence of the rotor is apparent by the number of blades, blades aerodynamics such as stall or attached flows, tip vortices, etc. The helical vortices induced by the rotating blades are another important parameter of the near wake. The evolution of helical vortices is responsible for the behavior of the turbulent wake flow structures behind the wind turbines. The tip vortices are an important contributor to noise generation and blade vibration (Massouh and Dobrev 2007). The far wake is the region behind the near wake, where the actual rotor shape is less important, but the focus is on wake modeling, wake interference in wind farms, turbulence modeling, and topographic effects (Vermeer et al 2003).

Deep-water offshore environments are characterized by strong wind speeds (due to shallower boundary layer profiles), and lower turbulence intensities (due to smoother surface roughness of offshore environments). Generally, the higher and steadier wind speeds would result in higher energy production. The reduced ambient turbulence of offshore environment will help in reducing the fatigue loads on wind turbine components. But, reduced ambient turbulence will also reduce the entrainment of the turbulent kinetic energy (T.K.E.) from the high energy flow above, and therefore, it causes the wake to travel longer. Hence, the spacing between the offshore turbines may need to be larger in comparison to that of onshore wind turbines. On the other hand, the effect of the floating motion on offshore wind turbine aerodynamics can be thought of as a stationary turbine operating in a highly unsteady and fluctuating flow. Therefore, it is anticipated that these motions would have significant influence on the mechanically generated turbulence in the wake of the floating turbine, hence, impacting the entrainment of the T.K.E. in the wake and thus affecting the distance required between the offshore wind turbines.

Stanislav et al. performed a wind tunnel experiment to observe the influence of the platform pitch on the wake of a wind turbine. His results indicated that the platform pitch creates an upward shift in all components of the flow and their fluctuations. He concluded that the vertical flow created by the pitch motion as well as the reduced entrainment of kinetic energy from undisturbed flow above the turbine result in potentially higher loads and less available kinetic energy for a downwind turbine.

Sebastian et al. performed series of numerical simulations on floating wind turbines, and determined that the blade element momentum theory does not capture the unsteadiness generated in the flow due to significant changes in the angle of attack. Large angle of attack changes were due to the additional motion of the floating platforms.

Motion induced unsteadiness violates assumptions of standard blade element momentum theory and leads to inaccurate predictions of unsteady aerodynamic loads. He showed that pitching motion of the wind turbine causes the turbine to change from the windmill state to the propeller state.

The similitude law using Froude scaling, used widely in hydrodynamic studies, was also used in the current wind tunnel study. With only few numerical work known in the literature, and even fewer experimental work done on the subject of floating wind turbines, there are still confusions as for which similitude law should be adopted to perform wind tunnel experiments on floating offshore wind turbines (FOWT). Therefore, many researchers across engineering disciplines who know that matching Reynolds number in a wind tunnel study is not an option, argue to match the Froude number instead. This paper presents the results of wind tunnel testing on a wind turbine model subjected to surge motion using the Froude scaling method.

## II. Experimental Setup

The present experimental study is performed in the large-scale Aerodynamic/Atmospheric Boundary Layer (AABL) wind and gust tunnel located in the Department of Aerospace Engineering at Iowa State University. The AABL wind tunnel is a closed-circuit wind tunnel with a boundary-layer test section 20 m long, 2.4 m wide and 2.3 m high, optically transparent side walls, and with a capacity of generating a maximum wind speed of 40 m/s in the test section. Arrays of chains were laid-out on the wind tunnel's floor on the upstream side of the wind turbine model in order to match the flow to that of offshore environment. The boundary layer growth of the simulated ABL wind under almost zero pressure gradient condition was achieved by adjusting the ceiling height of the test section of the wind tunnel. The oncoming boundary layer wind velocity profile was fitted by using equation 1, where  $z_{ref}$  is a reference height (hub) and  $U_{ref}$  is the wind speed at the reference height. The power law exponent ' $\alpha$ ' is associated with the local terrain roughness. Figure 1, shows the measured streamwise mean velocity (normalized with respect to the hub height velocity,  $U_{hub}$ ) and the turbulence intensity profiles of the oncoming flow in the test section for the present study. The power law exponent of in Eq. 1 was found to be  $\alpha = 0.10$ , corresponding to the open sea boundary layer profile according to the Japanese standard (AIJ or Architecture Institute of Japan). GL (Germanischer Lloyd) regulations define a turbulence intensity of 0.12 at the hub height of offshore wind turbines; however, this value was determined to be very conservative compared to field measurements. Therefore, for the current experimental study, a turbulence intensity of 10% at the hub height of the model turbine was chosen.

$$U(z) = U_{ref} \left( \frac{z}{z_{ref}} \right)^\alpha \quad (1)$$

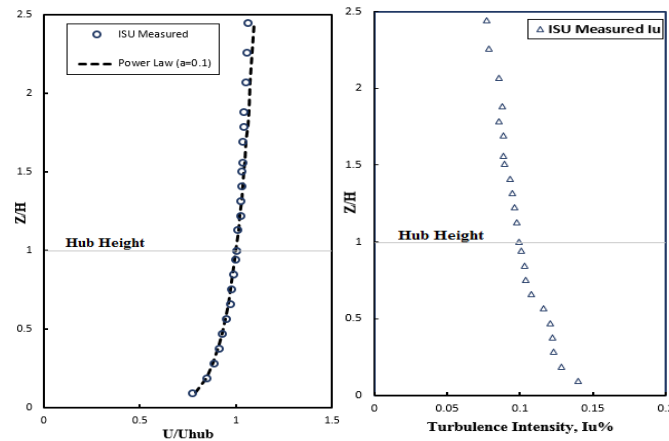


**Figure 1: Atmospheric boundary layer profiles**

The energy spectrum of the wind contains various information about the flow and relevant to wind turbine studies. The area under the curve represents the turbulence intensity at the hub height of the turbine. As shown in Fig. 2, the power spectrum curve of the stream-wise turbulence as estimated from measurements is compared with the well-known Kaimal spectrum where the results show a high degree of consistency between the two spectra. The closeness of the two curves will ensure that the type of turbulent eddies expected on the model will be proportionately smaller at the same length scale (model scale) as the turbulent eddies experienced by the actual turbine.

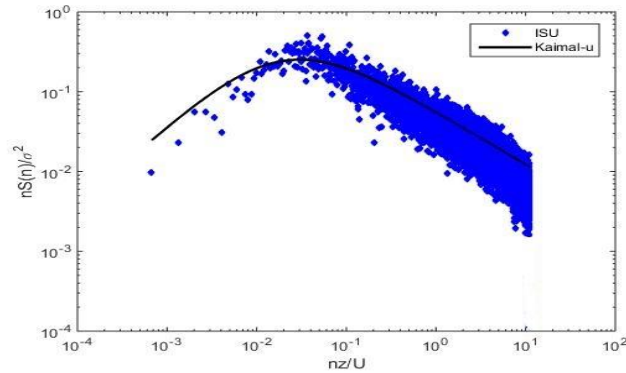


**Figure 2: The measured power spectrum curve**

As shown in Fig. 3, a 1:300 geometrically scaled model horizontal axis wind turbine (HAWT) with a hub height of 270 mm and rotor diameter of 300 mm was developed using rapid prototyping method. The rotor blades were designed based on the ERS-100 prototype turbine blades developed by TPI Composites, Inc. The rotor blade has a constant circular cross section from the blade root to 5% blade radius (R), and three NREL airfoil profiles (S819, S820, S821) are used at different spanwise locations along the rotor blade. The S821 airfoil profile is used between 0.208R and 0.40R, the S819 primary airfoil is positioned at 0.70R, and the S820 airfoil profile is specified at 0.95R. For optimized performance of the rotor, the blades were pitched by 3 degrees.

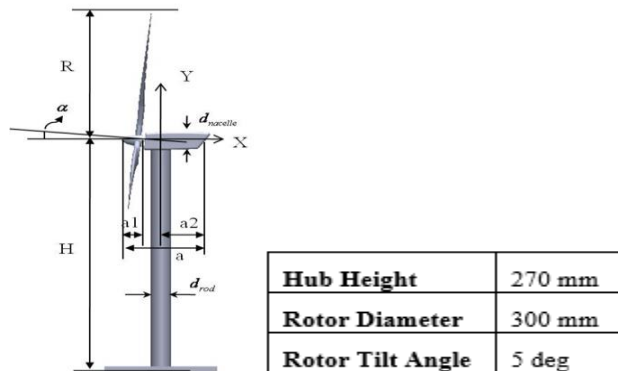


**Figure 3: The design parameter of the model turbine**

The blockage ratio was calculated to be around 1.3%, which is well within the acceptable range. An M-ILS150cc high precision linear stage motion simulator device manufactured by Newport Corporations is used to replicate the surge motion of a floating wind turbine. As shown in Fig. 4, the motion simulator device was carefully installed under the test section floor of the wind tunnel to avoid any flow disturbances due to the presence of such device. The turbine was then placed on top of the motion simulator through a special cut in the tunnel's floor.

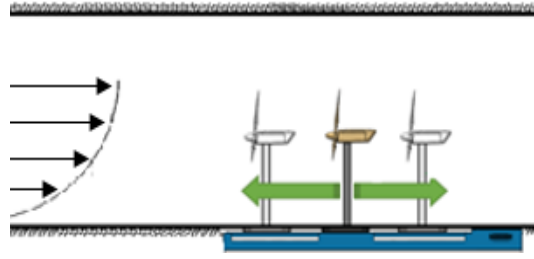


**Figure 4: Illustration of the wind tunnel test section with turbine and motion simulators installed.**

Besides matching the classical tip-speed-ratio (TSR) between the model and the prototype wind turbine, other scale relationships must also be maintained when dealing with floating wind turbines (Martin et al, 2012). By using Froude scaling, the wave forces and response of the floater will be correct (ignoring the scale effect in viscous forces). The wind loads on the turbine should also be scaled using Froude scaling, otherwise the floater motions will not be correct. In hydrodynamic testing, this is achieved by calibrating the correct wind forces, rather than the correct wind velocity. Therefore, once the Froude scaling is applied to the wind velocity, further adaptation of wind velocity will be required in order to achieve an acceptable thrust load on the turbine.

$$TSR = \frac{\Omega R}{U_{\infty}} \quad (2)$$

Where  $\Omega$  is the angular velocity of the turbine in rad/s, and  $U_{\infty}$  is the mean free-stream velocity at the hub height of the turbine.

$$Fr = \frac{U^2}{gl} \quad (3)$$

Froude number is the ratio between the inertial to gravitational forces, where  $U$  is the velocity of the fluid,  $g$  is the acceleration due to gravity, and  $l$  is a characteristic length.

$$\lambda_U = \sqrt{\lambda_l} \quad (4)$$

By applying Froude scaling, Eq. (3) becomes (4), where  $\lambda$  is a scaling factor. From (4), the calculated hub height wind speed becomes below 1m/s. At this wind speed, the model turbine would not operate. Therefore, to ensure the turbine is operating, and in order to achieve an acceptable thrust coefficient ( $C_T$ ) of 0.4 the free-stream velocity was increased to achieve a 5.7 m/s at the hub height of the turbine. The exact motion of the turbine was determined using the previous numerical simulation results and by applying Froude scaling on floating wind turbines done by Sebastian et al. The turbine was oscillating along the surge motion with a range of 2 cm forward and backward from the neutral location and with a frequency of 0.18 Hz.

### III. Results and discussion

A small DC motor (Kysan, FF-050S-07330) was mounted in the nacelle and operated as a generator which would produce electricity as driven by the rotating blades. To allow the wires from the nacelle to pass through the tower and connect to the measurement systems, a hollow aluminum rod was chosen as the turbine's tower. The significantly lower power production of the small model wind turbine was attributed to the low operating range of

Reynolds number that can be achieved in the wind tunnel. The efficiency of the motor also plays an important role in the low power extraction by the small DC motor. The corresponding diameter based Reynolds number ( $Re_D$ ) for this experiment was  $1.2 \times 10^5$  which was found to be much lower than the large scale wind turbines operating in the fields. However, the main flow statistics (mean velocity, turbulence intensity, kinematic shear stress, and velocity skewness) become independent of Reynolds number starting from  $Re \sim 93000$  (Chamorro et al. 2011). The tip speed ratio was measured to be 5, which is quite similar to what we see in a full scale wind turbine. Nevertheless, as shown in Fig. 5, the power extracted by the turbine during the surge motion was increased by 1% when compared to the bottom fixed turbine.

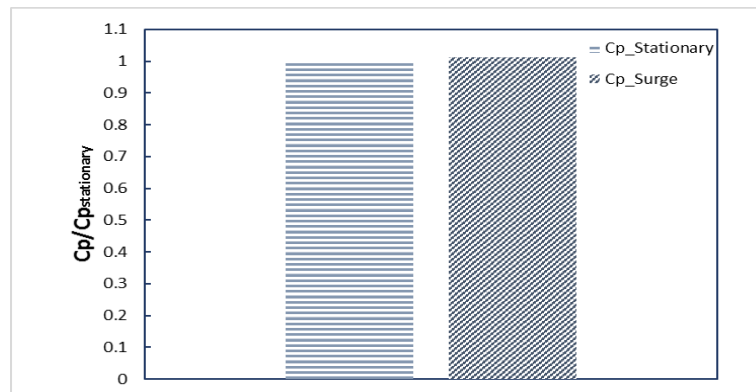


**Figure 5: Comparison between the power coefficients in surge motion and stationary turbine, normalized with respect to the stationary turbine.**

Particle Image Velocimetry (PIV) technique was used to obtain detailed flow field measurements in the near wake ( $X/D < 2$ ) of a fixed and a moving turbine in order to assess the turbulent near wake flow structure characteristics. Fig. 8, shows the PIV experimental set-up installed in the AABL wind tunnel. The seeded particles (oil droplets from smoke generator) in the airflow were illuminated by a double-pulsed Nd:YAG laser on XZ plane ( $Y/D=0$ ). The thickness of the laser sheet in the measurement regions was about 1.5 mm, and one 2k\*2k pixel CCD camera was used to capture the PIV images on the two measurement regions with an overlapping region of 25 mm length. The CCD camera and the double-pulsed Nd:YAG laser were connected to a host computer via a digital delay generator so that the timing between laser illumination and image acquisition could be adjusted.

After Image acquisition, instantaneous PIV velocity vectors were obtained by frame to frame cross-correlation. An interrogation window of 32\*32 pixels was employed for each successive frame patterns of PIV images with an effective overlap of 50%. Then, the ensemble averaged flow quantities such as normalized velocity ( $U/U_{hub}$ ), normalized Reynolds stress ( $R_{uv}/U_{hub}^2$ ) and normalized Turbulent Kinetic Energy ( $TKE/U_{hub}^2$ ) were obtained from approximately 1000 frames of instantaneous PIV measurements.



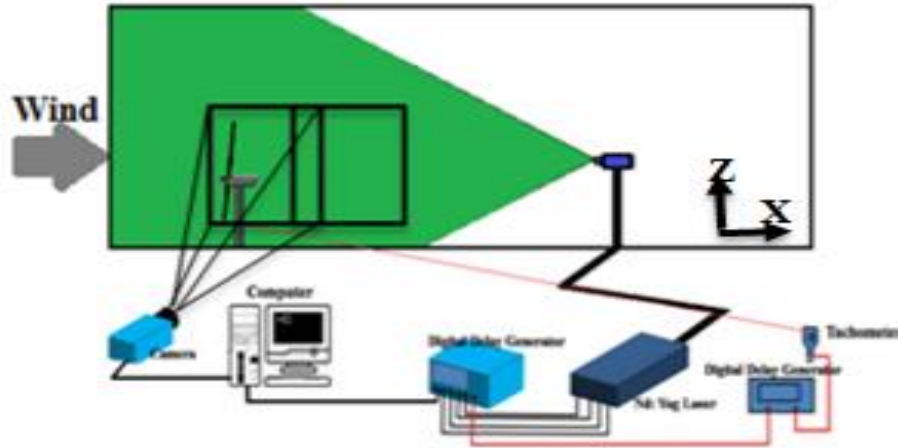


**Figure 6: Schematic of the PIV set-up**

Fig. 9 shows contours of the ensemble-averaged normalized streamwise mean velocity  $U/U_{hub}$ , for the turbine in surge motion and the stationary turbine. The following measurements were taken only when the turbine base passed the center or the neutral location of the cyclic surge motion. In order to better understand the full effect of the surge motion, the motions were divided depending on which direction the turbine was moving. From the measurements, there is clear evidence of deficit in the velocity profiles in the wake of the turbine, which is the result of energy extraction by the turbine itself. Double peaks are observed and understood as characteristic of the near wake profiles. But as we go farther down in the wake, the double peak becomes just a single peak. This single peak eventually dies out in approximately 15~20 diameter downstream of the turbine, where the flow gains its fullest momentum and becomes the free-stream flow again. There is some overshoot at the top region of the profile which suggests that the flow is accelerating at near the top-tip of the blade, and also could be an evidence of the blockage effect caused by the existence of the turbine itself. As can be seen in plots of Fig. 7, as the turbine oscillates about the neutral location, it captures slightly more energy from the flow, in comparison to when the turbine is fixed in place. These results are quite consistent with the power extraction results from the DC motor as shown before. The direction of motion did not make any significant difference in the velocity profiles in the wake.

The turbulent kinetic energy (T.K.E.) is the kinetic energy associated with turbulent flows per unit mass. By studying the TKE, one can determine on how fast the wake is recovering. The fluctuating components of the oncoming boundary layer flow influences the turbulent wake flow structure significantly. For a uniform flow, mean shear distribution in the turbine wake could be axisymmetric with strong shear layer (associated with TKE production) at the levels of bottom-tip and top-tip. However, for an oncoming boundary layer flow with non-uniform mean flow velocity distribution, previous experimental and numerical studies showed that maximum TKE production would occur at the top-tip level as a result of strong shear-produced turbulence and turbulence (momentum) fluxes (Hu et al., 2012; Zhang et al., 2012; Porte-Agel et al., 2011; Wu et al., 2012). Turbulent fluxes produced due to wake induced turbulence were found to play an important role on the entrainment of energy from the flow above the wind farm (Meyers and Meneveau, 2013). Fig. 8 shows the contour and the corresponding plots of the  $TKE/U_{hub}^2$  for the surge motion and the stationary turbine. Slight increase of TKE was observed only near tip-top of the blade, but otherwise there is little difference in TKE of the surge motion and the stationary case. Reynolds shear stress plots are also shown in Fig. 9. The Reynolds shear stress deals with the amount of high energy momentum from the undisturbed flow above the turbine that is being transported into the wake region. Hence, directly influencing how fast the wake is recovering.

As can be seen in Fig. 9, there is significant reduction in the Reynolds shear stress associated with the floating case, which can suggest that the recovery rate of the wake would be much slower in comparison to the bottom fixed turbine.

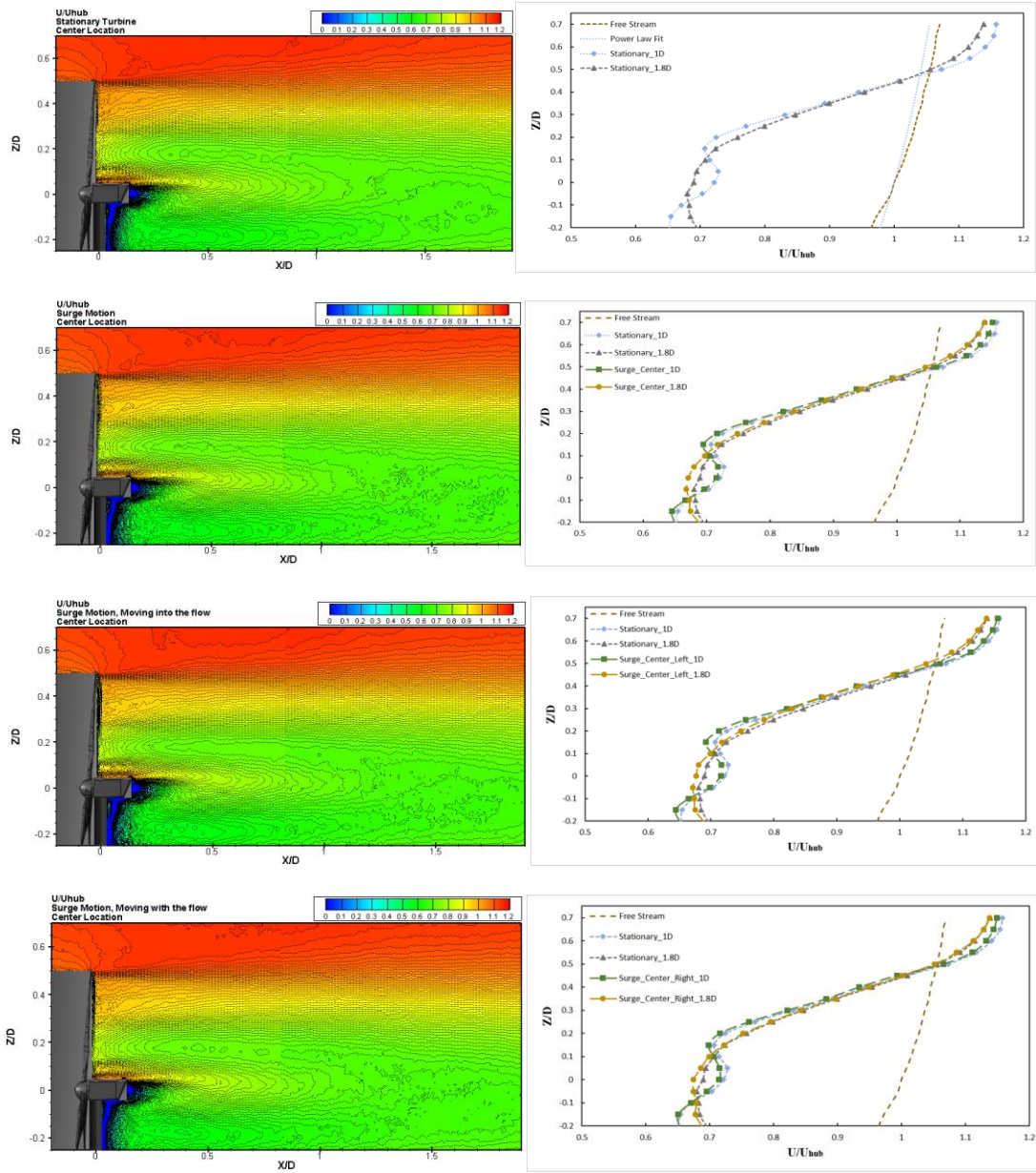


**Figure 7: The contour and plots of the ensemble-averaged normalized stream-wise mean velocity for stationary turbine, and center location for surge motion.**



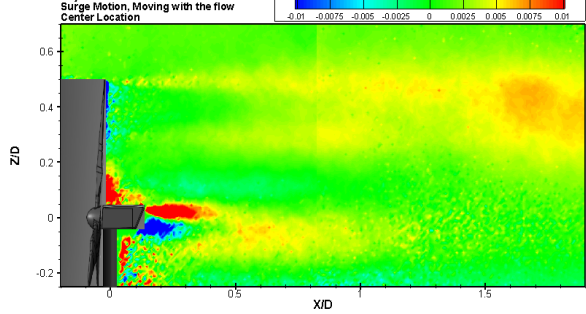
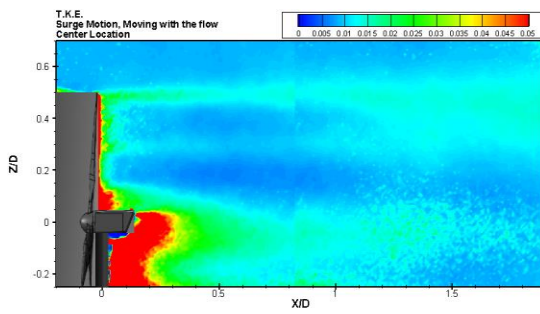
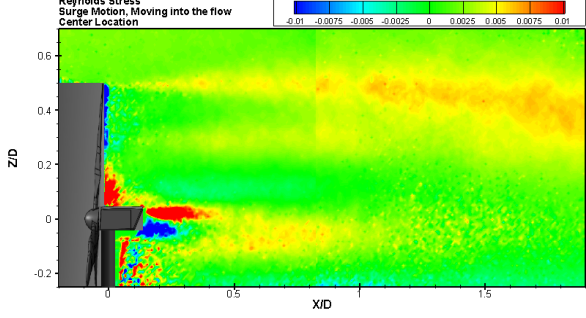
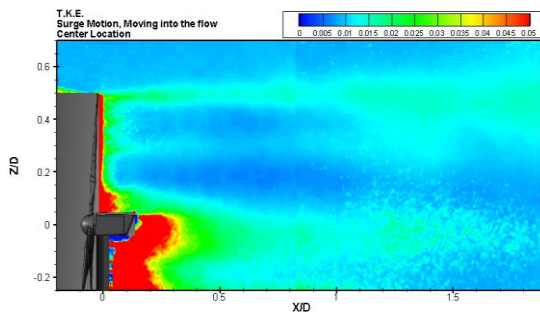
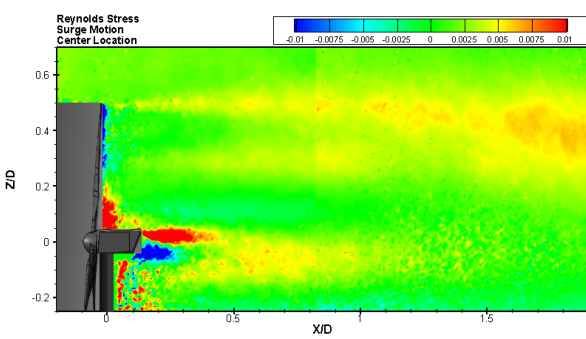
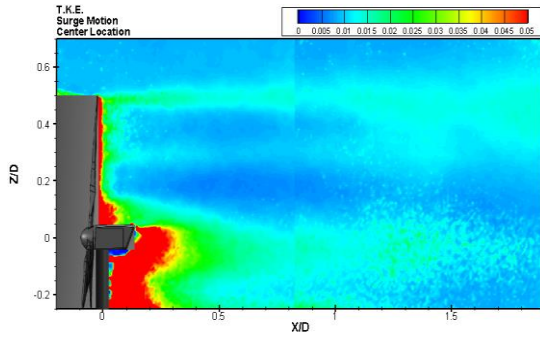
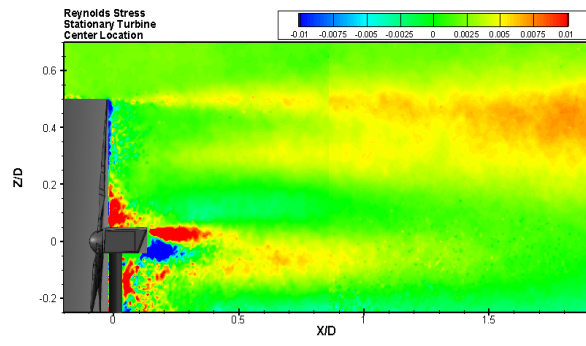
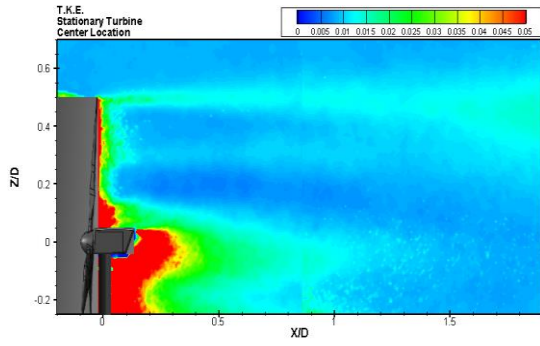


**Figure 8.** The contours of the ensemble-averaged normalized TKE production ( $TKE/U_{hub}^2$ ), in the near wake of the surging and stationary turbines.

**Figure 9:** The contours of the ensemble-averaged Reynolds shear stress ( $R_{uu}/U_{hub}^2$ ), in near wake of the surging and stationary turbines.

#### IV. Summary and conclusions:

Offshore floating wind turbines are the future of wind energy (Sebastian et al., 2012). The United States is especially fortunate to be surrounded by vast yet deep waters on both east and west sides of the nation. This provides a unique opportunity for offshore floating wind farm developments in USA. But, so far, no major progress has been made in developing any offshore floating wind farms. This is mainly due to lack of experience and knowledge needed to overcome the obstacles faced by offshore wind turbine development. One of these obstacles is the uncertainty associated with the performance of such floating turbines. With only few numerical simulation studies being done to understand the coupled behavior of floating offshore wind turbines, there is a need for a comprehensive experimental study to validate the numerical results and perhaps to improve our current understanding of the floating offshore wind turbines' performance and aerodynamics, which can potentially lead to more accurate load and performance predictions and design improvements.

In order to understand, and fully explore the aeromechanics behavior of a floating wind turbine, a comprehensive experimental study was conducted on a wind turbine subjected to surge motion only. The results were then compared to that of a traditional bottom fixed turbine. A high resolution PIV system was used for detailed near wake flow field measurements (free-run) so as to quantify the near wake turbulent flow structures. The results reveal that the power produced by the turbine moving in surge motion is approximately 1% higher than the stationary turbine. The loading measurements also suggest that thrust load as well as the vertical load at the base of the moving turbine were decreased in comparison to that of the stationary turbine. Furthermore, a reduction in the Reynolds shear stress was also noted in the case of the surge motion, which suggests that the wake of the moving turbine in surge motion will be traveling longer before it dissipates, hence the required distance between offshore wind turbines (FOWT) will need to be larger in comparison to the traditional bottom fixed turbines.

This study was the first part of a series of experiments that are being conducted to fully understand the contribution of each motion along each DOF's to the overall performance, loading, and the wake characteristics of floating offshore wind turbines. The method employed in this study was based on Froude scaling. Although, applying Froude scaling is a preferred method in hydrodynamic testing, but the results of the wake study of floating turbine show little difference when compared to the stationary turbine, hence suggesting that the Froude scaling may not be the appropriate method when dealing with aerodynamics studies. A second method based on maintaining the ratio of the surge motion to the freestream wind speed is also under investigation. It is anticipated that the ratio method to be able to accurately capture the statistics in the wake due to the motion of the turbine itself.

## References

- Chamorro, L. P., Porte-Agel, F. (2009). A wind-tunnel investigation of wind-turbine wakes: boundary layer turbulence effects. *Boundary Layer Meteorol* 132:129–149
- Corbetta G. 2014, The European offshore wind industry key trends and statistics 1st half 2014, European Wind Energy Association
- Hu, H., Yang, Z., Sarkar, P., (2012). Dynamic Wind Loads and Wake Characteristics of a Wind Turbine Model in an Atmospheric Boundary Layer Wind. *Experiments in Fluids* 52(5):1277-1294.
- Martin H.R., 2011, Development of a Scale Model Wind Turbine for Testing of Offshore Floating Wind Turbine Systems, M.S. Thesis, University of Maine, Orono.
- Massouh H, Dobrev I (2007) Exploration of the vortex behind of wind turbine rotor. *J Phys Conf Ser* 75:012036
- Musial W., Ram B., 2010, Large-Scale Offshore Wind Power in the United States, Technical Report NREL/TP-500-40745.
- Porte-Agel, F., Wu, Y. T., Lu, H., Conzemius, R. J. (2011). Large-eddy simulation of atmospheric boundary layer flow through wind turbines and wind farms. *Journal of Wind Engineering and Industrial Aerodynamics*, 99, 154–168.
- Rockel, S.; Camp, E.; Schmidt, J.; Peinke, J.; Cal, R.B.; Hölling, M. Experimental Study on Influence of Pitch Motion on the Wake of a Floating Wind Turbine Model. *Energies* 2014, 7, 1954-1985.
- Sebastian, T.; Lackner, M. Characterization of the unsteady aerodynamics of offshore floating wind turbines. *Wind Energy* 2013, 16, 339–352.
- Vermeer, L. J., Sørensen, J. N., Crespo, A. (2003). Wind turbine wake aerodynamics. *Progress in Aerospace Sciences*, 39, 467–510.
- Wu, Y. T. & Porte-Agel, F. (2012). Atmospheric turbulence effects on wind-turbine wakes: An LES study. *Energies*, 5, (12), 5340–5362.
- Zhang, W., Markfort, C. D., Porte-Agel, F. (2012). Near-wake flow structure downwind of a wind turbine in a turbulent boundary layer. *Experiments in Fluids*, 52, 1219–1235.